IRSTI 29.17.01, 55.49.03 https://doi.org/10.26577/ijmph.20261717

NUMERICAL STUDY OF GIMBAL JOINT GAP INFLUENCE ON NOZZLE FLOW

A.S. Toleubay [1], M.K. Omarbayev [1], T.K. Zhakenova [1], N.M. Spandiyar [1], A.Y. Dintayev [1], M.K. Suleimenov [1] and A.Y. Komekbayev [2]

[1] *JSC National Center for Space Research and Technology, Almaty, Kazakhstan*

[2] *Almaty University of Energy and Communications named after Gumarbek Daukeev, Almaty, Kazakhstan*

Email: aruzhantoleubay4@gmail.com

(Received 5 April 2026; revised 15 May 2026; accepted 20 May 2026)

Abstract. Gimbaled thrust vector control (TVC) systems are widely employed in modern launch vehicles to provide attitude control during powered flight. However, the aerodynamic influence of the circumferential geometric discontinuity introduced by the gimbal joint gap on nozzle internal and external flow remains insufficiently studied in open literature. The purpose of this study is to evaluate aerodynamic losses and flow field modifications of bell-shaped rocket nozzles with the presence of a gimbal joint gap using computational fluid dynamics (CFD) simulation. These calculations were done using the Reynolds-Averaged Navier–Stokes (RANS) model in 2D axisymmetric flow in ANSYS Fluent software. For modelling the flow properties in compressible separated flows, the k-ω SST turbulence model was selected. Two nozzle configurations, with and without the gap of the gimbal joint, were compared. The Sutherland viscosity law and the NASA polynomial thermodynamic data were used for the working fluid and it was modeled as an ideal compressible gas representative of the combustion products of LOX/Kerosene. The exit to throat area expansion ratio for nozzle geometry is 8.97, which means that the nozzle is designed to have a supersonic exit condition. The CFD results showed a good agreement with the theoretical results, showing the validity of the numerical approach. The nozzle studied here operates under overexpanded conditions at sea level, where the nozzle exit static pressure falls below ambient pressure, giving rise to oblique shock waves in the exhaust plume and making the accurate characterisation of flow disturbances particularly important. The presence of the gimbal joint gap was found to introduce aerodynamic losses in Mach number of 6.74%, providing quantitative design-relevant data for gimbaled nozzle systems in launch vehicles.

Keywords: gimbal joint gap, bell nozzle, TVC, CFD

INTRODUCTION

Rocket nozzle flow dynamics are of fundamental importance in propulsion engineering as they directly impact thrust performance, efficiency, and operational stability of liquid propellant rocket engines (LPREs). Rocket nozzles generate thrust by expanding and accelerating high-pressure, high-temperature combustion products into a directed supersonic jet [1, 2]. Very light-class launch vehicles have small upper stages that impose strict requirements on all subsystems for minimal dimension, high reliability and functional completeness [3].

The ability to accurately direct the thrust of rocket nozzles is essential to mission success. Thrust Vector Control (TVC) systems enable this by deflecting the exhaust jet, allowing the vehicle to maneuver and maintain attitude stability throughout the powered flight phase. Effective TVC is therefore an essential component of modern launch vehicles and aerospace propulsion systems [4]. Among the different TVC techniques, the gimbaled nozzle remains the most widely used mechanism in liquid-propellant rockets. In this configuration, the entire nozzle assembly is mounted on a pivoting joint that allows angular deflection about one or two axes. By introducing a gimbal angle δ, the thrust vector is redirected, generating a lateral force component that enables effective control of the rocket's attitude during flight [5].

TVC nozzle flow research experiments provide useful data but involve significant technical and economic challenges. Physical studies are limited due to high operating costs, the need for near vacuum conditions and the inability to du-

plicate these conditions in ground-based facilities. The use of Computational Fluid Dynamics (CFD) is very useful in the development process as full scale experiments of the rocket engine elements are quite expensive and time consuming [6]. Reynolds-Averaged Navier-Stokes (RANS) simulation with the k-ω SST turbulence model has been demonstrated to be accurate in predicting wall pressure distribution and shock structure for internal nozzle flows and supersonic plumes, and is appropriate for parametric studies [6]. However, despite the prevalence of gimbal nozzle systems in the rocket industry, the aerodynamic influence of the gimbal joint gap geometry on the nozzle flow field has received limited attention in the open literature.

The ambient pressure environment experienced by a rocket nozzle changes drastically over the course of a typical mission. The nozzle is located at sea level and during the lower atmospheric flight phase, the ambient pressure at the nozzle is around 101,325 Pa. In this case, a nozzle with a high area ratio will operate in the overexpanded regime in which the static pressure at the nozzle exit will be lower than ambient pressure, and oblique shocks, flow separation, and sideload generation may occur [7, 8]. Understanding nozzle flow behavior across this regime is essential for the design of multi-stage launch vehicles. Studies combining bell nozzle aerodynamics, gimbaled TVC, and gap effects are sparse. Available investigations mostly address gimbaled nozzles at the system level and gap clearance effects in other TVC schemes, often in converging-diverging nozzles [9, 10]. In addition, the presence of a gap between the tab and the nozzle exit plane has been shown to affect the recirculation-zone position. As the gap size increases, the separation point moves closer to the nozzle exit plane, while the plateau pressure decreases due to gas leakage through the gap. This suggests that the separated-flow structure and the pressure distribution can be greatly modified by the geometry of the gaps, and thus a detailed investigation of gimbal-gap effects in rocket nozzles is still needed [11].

Although numerous research projects are currently underway in the field of rocket nozzle aerodynamics and thrust vector control (TVC) systems, the local aerodynamic effects generated by the gimbal gap are not well understood. Specifically, there is a need for detailed quantitative analysis identifying the effect of this geometric discontinuity on the internal flow structure, the wall pressure distribution, the plume development and on the overall thrust performance under different ambient conditions. Given that even small perturbations in high-speed compressible flow can lead to significant performance losses, a systematic investigation of this effect is necessary. Furthermore, most existing studies focus either on idealized nozzle geometries or on global system-level behavior, without resolving the local flow phenomena associated with structural discontinuities such as gaps. As a result, the aerodynamic penalties associated with the gimbal gap are often neglected or underestimated in the design process of gimbaled nozzle systems.

In this application, Computational Fluid Dynamics (CFD) is a very useful tool for solving complex flow phenomena that cannot be easily observed experimentally [6, 7]. High fidelity numerical simulations can be used to study the interaction of shock structures, boundary layers and geometrical irregularities and to evaluate the combined effect on nozzle performance. Based on that, the aim of this research is to study numerically the effect of the gimbal gap on the internal and external flow characteristics of a bell-shaped rocket nozzle in an atmospheric condition by simulating the flow using a 2D axisymmetric RANS model. The novelty of this work is the comparison of nozzle configurations with and without a gimbal gap under the same operating condition, mesh topology and physics model, which would allow a legitimate and direct estimation of the aerodynamic effect of the gap. The results give insight into the flow disturbances, the shock behavior, the thrust performance and the flow field characteristics of the thrust vector control system with geometric feature, such as flow velocity, flow temperature, flow pressure distribution etc.,

which is useful for designing and optimizing the rocket propulsion system with thrust vector control system.

Materials and Methods

Geometry, Computational Domain, and Boundary Conditions

A two-dimensional axisymmetric model of a bell-shaped rocket nozzle was considered in this study. The nozzle geometry is characterized by a converging–diverging profile designed for supersonic flow expansion. Geometrical parameters of the nozzle include the throat radius of 13.14 mm, the exit radius of 39.36 mm, and the ratio of exit to throat area of around 9.

To investigate the influence of the thrust vector control system, a geometric discontinuity representing the gimbal joint gap of 0.4 mm was introduced into the nozzle wall. For reference, this value is consistent with sub-millimeter gap heights reported in fluidic thrust vectoring studies, where gaps in the range of 1–2 mm have been shown to directly influence the thrust vectoring angle [12], and smaller gaps are expected in gimbaled rocket nozzle hardware due to more stringent leakage and structural constraints.

The computational domain consists of both the internal nozzle region and the external flow field downstream of the nozzle exit. The external domain was extended to 16.1 times the nozzle exit diameter in the radial direction and 8.15 times the nozzle length in the axial direction downstream of the exit plane, ensuring that boundary effects do not influence the flow solution within the region of interest. The domain dimensions were chosen to be large enough to achieve the complete evolution of the exhaust plume, and numerical stability and accuracy.

The computational domain and the boundary conditions used in the numerical simulation of the bell nozzle flow are shown in Fig. 2. The nozzle geometry was considered to be axisymmetric, enabling the use of a 2D model to benefit from the geometry while capturing the essential characteristic aspects of the internal and external flow fields.

At the inlet, corresponding to the chamber entrance, a mass flow inlet boundary condition was applied. The inlet mass flow was specified as 8.78 kg/s, with a total temperature of 3000 K. The total pressure at the inlet was set to 6.75 MPa. A turbulence intensity of 5% and a hydraulic diameter equal to the inlet diameter were specified at the inlet boundary condition to define the incoming turbulence length scale, consistent with the recommended practice for internal combustion-driven flows in ANSYS Fluent. It was assumed that the flow properties at the inlet remain uniform, which guarantees a uniform inlet and provides numerical convergence. The walls of the nozzle were represented by a no-slip boundary condition, thereby considering the influence of the viscous effects which are present in the near-wall region. The assumption of an adiabatic wall condition was applied, where it is assumed that there will be no transfer of heat between the fluid and the surface of the nozzle.

The flow was axisymmetric and a symmetry boundary condition was used along the nozzle centerline to capture the three dimensional behavior in a two dimensional solution. At the outlet, a pressure outlet boundary condition was specified. One pressure condition was considered to simulate flight regime. For the overexpanded flow case, corresponding to sea-level operation, the outlet pressure was set to atmospheric pressure (101,325 Pa). These boundary conditions enable an accurate representation of both internal nozzle flow and external plume expansion under atmospheric environmental conditions.

Mesh and Grid Independence

The computational mesh used for the numerical simulation was generated using ANSYS Fluent Meshing. Fig. 3 shows the computational mesh of the bell nozzle with gimbal joint gap: an overview of the full domain (bottom left) with a close-up view of the gimbal joint gap region showing local mesh refinement (top center). The medium mesh configuration with 1,012,018 cells was employed for all numerical simulations. A quadrilateral-dominant mesh with boundary layer

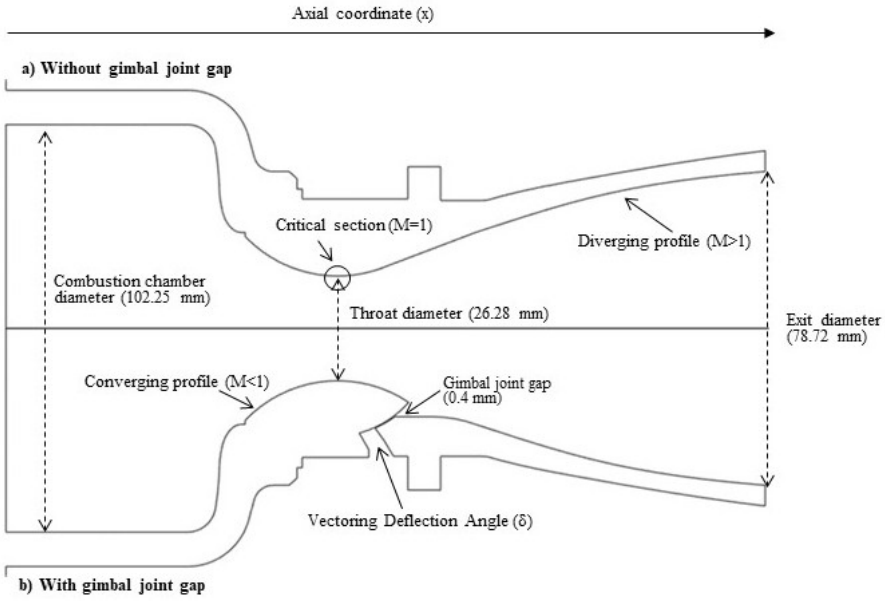

Figure 1 - Two-dimensional axisymmetric cross-sectional view of the bell nozzle geometry: (a) without gimbal joint gap and (b) with gimbal joint gap

inflation is applied along all wall surfaces, ensuring adequate resolution of near-wall flow features and viscous effects.

To ensure that the numerical results are independent of the spatial discretization, a mesh independence study was conducted prior to the main simulations. Three computational meshes of increasing refinement were generated for the baseline nozzle configuration without the gimbal joint gap under atmospheric conditions: a coarse mesh, a medium mesh, and a fine mesh. The key mesh parameters are summarized in Table 1.

Since the Mach number at the nozzle exit plane was one of the most important parameters that has a direct connection with the nozzle performance evaluation, it was used as the reference parameter for the mesh independence level evaluation. The differences in the exit Mach number between the coarse and the medium mesh were 0.19% and between the medium and the fine mesh were 0.13%, respectively, which meant the solution converged to be mesh independent. Thus, the medium mesh was chosen for all further simulations, which gets an optimum balance between computational accuracy and efficiency. For the selected mesh, the CFD-predicted exit Mach number of 3.776 was compared with one-dimensional isentropic theoretical value of 3.650, showing a difference of 3.17% which confirmed the spatial discretization for the present study.

Table 1 – Mesh independence study results.

Mesh type	Number of cells	Min. element size [mm]	Exit Mach No.
Coarse	259,137	0.2	3.758358
Medium	1,010,101	0.1	3.765603
Fine	3,989,159	0.05	3.770503

Governing Equations and Turbulence Model

The flow was simulated inside the rocket nozzle as a steady, compressible and turbulent flow with the Reynolds-Averaged Navier–Stokes (RANS) equations. The equations are the conservation of mass, momentum and energy for a viscous fluid.

The conservation of mass is described by the continuity equation:

$$\frac{\partial \rho}{\partial t} + \nabla \cdot (\rho u_i) = 0, \tag{1}$$

where ρ is the fluid density and u_i is the velocity

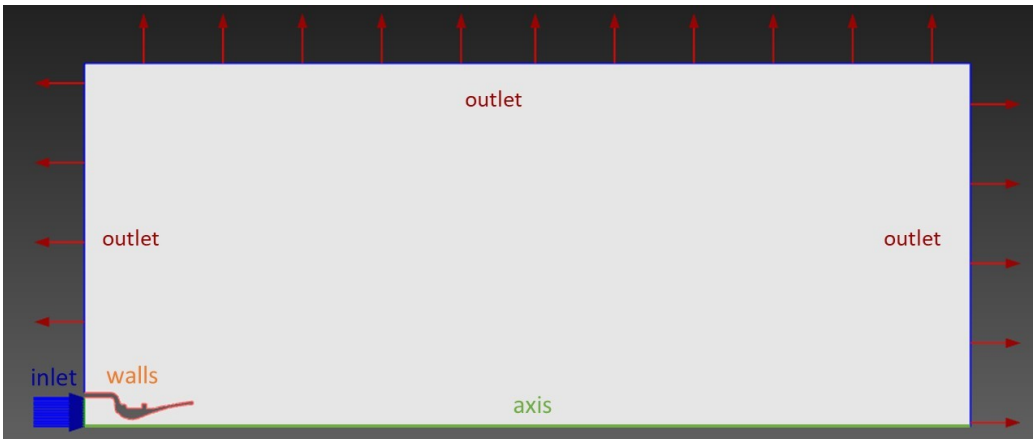

Figure 2 - Boundary conditions of the computational domain

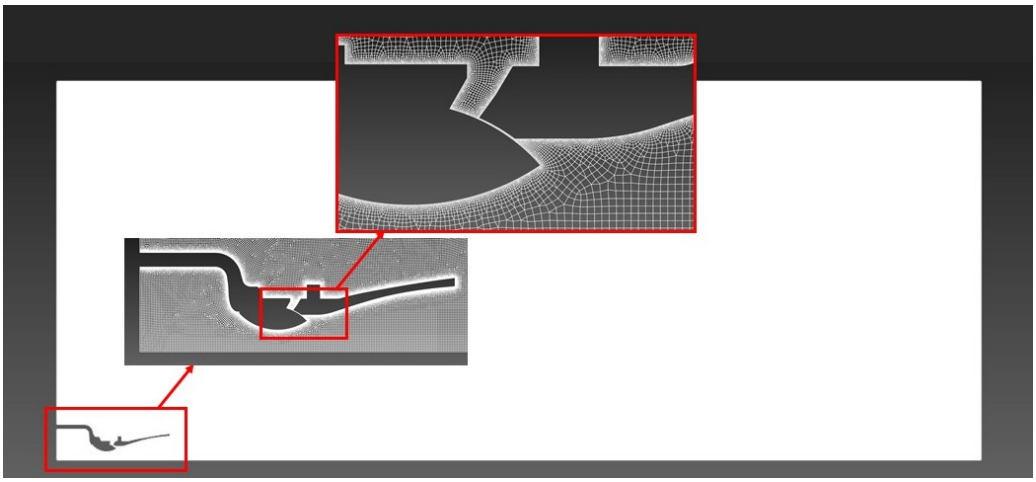

Figure 3 - Computational mesh

vector.

The conservation of momentum is expressed by the RANS momentum equation:

$$\frac{\partial(\rho\mathbf{u})}{\partial t}+\nabla\cdot(\rho\mathbf{u}\mathbf{u})=-\nabla p+\nabla\cdot(\mu\nabla\mathbf{u})-\nabla\cdot(\rho\overline{u'u'}), \quad (2)$$

where p is the static pressure, μ is the dynamic viscosity, and $-\rho\overline{u'u'}$ represents the Reynolds stress tensor generated by turbulent velocity fluctuations.

The conservation of energy is given by:

$$\frac{\partial(\rho E)}{\partial t}+\nabla\cdot\big(\mathbf{u}(\rho E+p)\big)=\nabla\cdot(k\nabla T)+\Phi, \quad (3)$$

where E is the total energy per unit mass, T is the temperature, k is the thermal conductivity, and Φ is the viscous dissipation.

The turbulence model is used to close the RANS equations to include turbulence effects. The k–ω Shear Stress Transport (SST) turbulent model was used in this study. This model has the benefit of being able to use the k–ω model close to solid surfaces and the k–ε model in free-stream regions and has been shown to be very effective in predicting flows with adverse pressure gradients and separation. The k–ω SST model is particularly suitable for high-speed compressible flows and has been widely used for predicting shock–boundary layer interactions, flow separation, and supersonic jet expansion.

The working fluid was modeled as a compressible ideal gas, and density variations were computed using the ideal gas equation of state:

$$\rho=\frac{p}{RT}, \quad (4)$$

where R is the specific gas constant. The thermodynamic properties were defined by NASA

polynomial 9 coefficients [13] and the viscosity of the gas was calculated using Sutherland's law [14] to represent the high-temperature gas accurately. The one dimensional isentropic flow relations were used for theoretical calculation of the Mach number.

Results and Discussion

The numerical results obtained were first compared with theoretical results to confirm the validity of the numerical model. The theoretical calculation of exit Mach number, using one-dimensional isentropic flow relations, was done for the area ratio of 8.97. The baseline design (gimbal gap absent) yielded a CFD calculated area-weighted average exit Mach number of 3.766 with a 3.17% error from the theoretical value. The degree of agreement shows that the numerical solution is a good approximation of the behavior of supersonic compressible flow in the nozzle.

The static pressure distribution along the nozzle axis for both configurations is shown in Fig. 4. The static pressure is approximately constant in the combustion chamber region ($x < -0.04$ m), as is consistent with the specified total pressure boundary condition. A sudden drop in pressure is seen in the throat area where the flow changes from subsonic to sonic. The pressure then drops further and the flow becomes supersonic in the diverging section, until it attains near-atmospheric pressure at the nozzle exit. The two configurations have almost the same pressure distribution in the convergent and throat region, which indicates that the gap of the gimbal joint has a negligible influence on the flow field upstream of the throat. In the configuration of the gimbal joint gap, however, a local pressure disturbance is noticed near the nozzle exit plane due to the interaction with the flow of the geometric discontinuity resulting in local flow separation and recirculation. A few geometric changes of nozzles, such as grooves or rings at the nozzle exit, can create large variations in flow separation, recirculation zones, turbulence intensity and operating conditions [15].

The Mach number distributions for both configurations are presented in Fig. 5. Under atmospheric pressure, the nozzle operates in an overexpanded regime, leading to the formation of oblique shock structures in the exhaust plume, clearly visible in the Mach number contours. If the flow is overexpanded, the flow detaches from the nozzle wall and oblique shock waves develop; for this, there are two distinct flow separation patterns: free shock separation and restricted shock separation, resulting in significantly different wall pressure distributions and flow structures [16, 17, 18]. For the configuration without the gimbal gap, the flow expands smoothly along the nozzle contour, with a uniform pressure distribution and a symmetric and stable plume structure.

In contrast, the configuration with the gimbal gap exhibits noticeable flow disturbances. The CFD-predicted area-weighted average Mach number and velocity at the nozzle exit for the configuration without the gimbal gap were 3.766 and 2328 m/s, respectively. With the introduction of the gimbal joint gap, these values were decreased to 3.512 and 2286 m/s respectively, or 6.74% in Mach number and 1.79% in exit velocity respectively. These reductions indicate that part of the flow energy is dissipated due to increased turbulence and flow separation induced by the gap geometry.

The static temperature and pressure profiles for both configurations are shown in Figs. 6 and 7, respectively. The temperature distribution is almost the same in the two cases as shown in Fig. 6. The high temperature exists mainly in the combustion chamber and decreases along the nozzle due to expansion; in the external flow, the overall distribution is virtually the same for both configurations. Likewise, no significant differences are noted between the two cases in the static pressure distribution, and there is no noticeable pressure discontinuity or strong pressure gradient in the vicinity of the gap.

The results indicate that the effects of the gimbal gap on the flow are mostly kinematic instead of thermodynamic. The effect on the flow direction and the local velocity distribution is

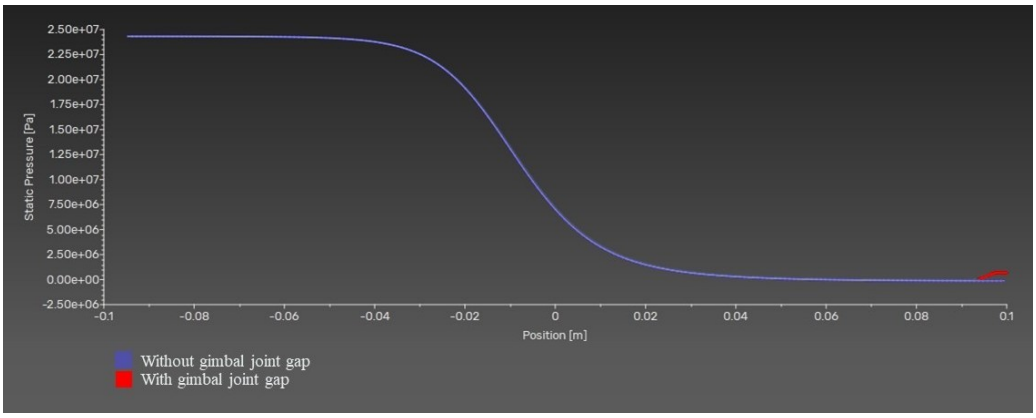

Figure 4 - Static pressure distribution along the nozzle axis for configurations with and without the gimbal joint gap under atmospheric conditions

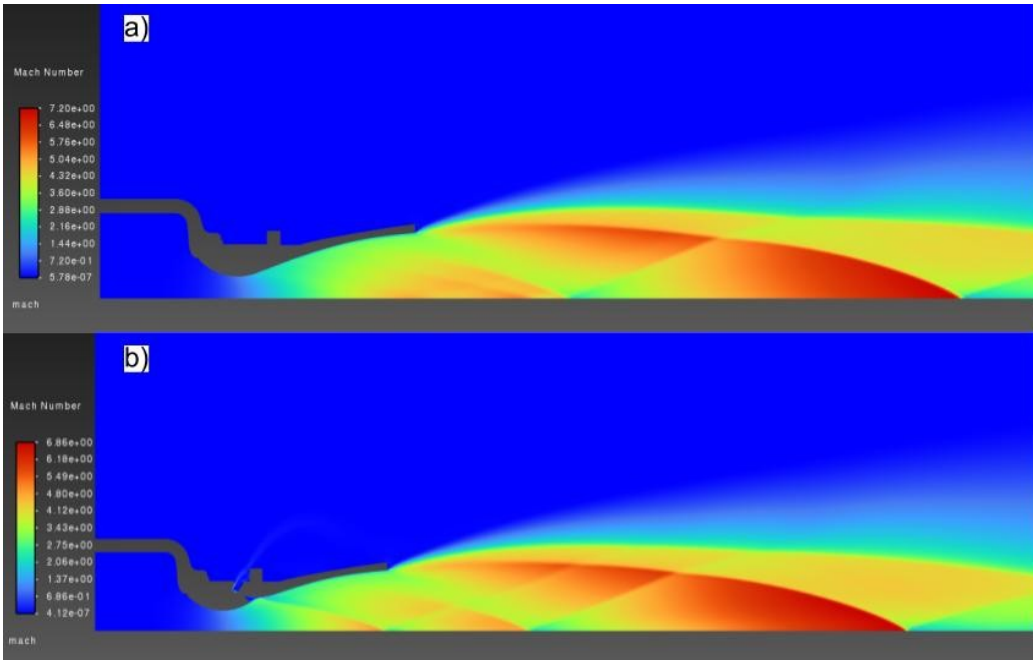

Figure 5 - Mach number distribution in the flow field for the nozzle under atmospheric conditions: (a) without gap, (b) with gap

measurable, but the effect on the global pressure and temperature fields is minimal, suggesting that the primary aerodynamic effect is due to the redistribution of momentum, and not the modification of the thermodynamic properties. From an engineering perspective, these results have direct implications for the performance of gimbaled nozzle systems in real launch vehicles. The observed 6.74% reduction in exit Mach number translates into a measurable decrease in effective exhaust velocity (c^* efficiency), which directly reduces the specific impulse (I_{sp}) of the rocket engine. For a LOX/Kerosene engine, a reduction of this magnitude in exit Mach number is estimated to correspond to a reduction in thrust coefficient C_f on the order of 2–4%, depending on the ambient pressure and nozzle operating condition. This in turn degrades the delivered thrust and, over a sustained burn, reduces the total velocity increment (Δv) available to the launch vehicle, a critical performance margin in the design of small upper stages, where mass and propellant budgets are tightly constrained. The results therefore demonstrate that the aerodynamic penalty associated with the

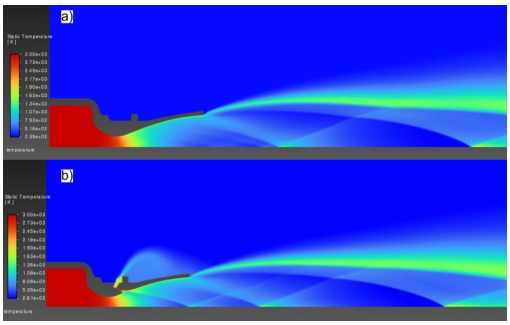

Figure 6 - Temperature distribution in the flow field for the nozzle under atmospheric conditions: (a) without gap, (b) with gap

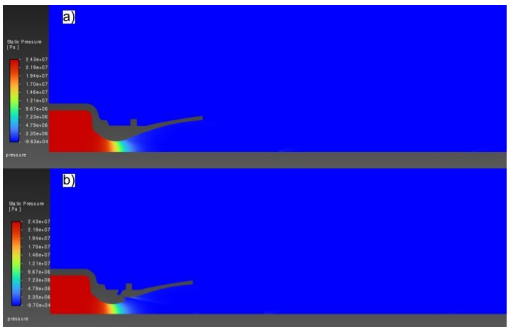

Figure 7 - Static pressure distribution in the flow field for the nozzle under atmospheric conditions: (a) without gap, (b) with gap

gimbal joint gap should not be neglected in the preliminary design and performance budgeting of TVC nozzle systems. Accounting for this loss may be particularly important for high-area-ratio nozzles operating at sea level in the overexpanded regime, where the interaction between the gap-induced flow disturbance and the existing oblique shock structures may amplify side-load generation and nozzle efficiency losses.

As observed in the velocity vector field (Fig. 8), the flow inside the gap region exhibits deflection and partial recirculation, confirming a loss of flow uniformity. The presence of the gap introduces a geometric discontinuity which causes the combustion gases to expand through the nozzle in a manner that is disrupted, causing a measurable reduction in the nozzle exit Mach number of 6.74%, which is aerodynamically significant for rocket propulsion applications where even small reductions in nozzle efficiency can have a significant impact on specific impulse and overall thrust performance.

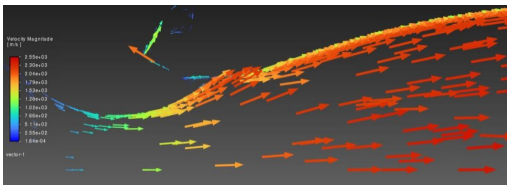

Figure 8 - Velocity vector distribution near the gimbal-gap region

CONCLUSIONS

In this paper, two-dimensional axisymmetric RANS simulation of a bell-shaped rocket nozzle with the k-ω SST turbulence model in ANSYS Fluent is used and the effect of the gimbal joint gap on the rocket nozzle flow characteristics is investigated numerically. The analysis was conducted under atmospheric ambient pressure conditions and based on the combustion gas properties of LOX/Kerosene with a molar mass of 24 g/mol and a total temperature of 3000 K, for two configurations: with and without a gimbal joint gap.

The CFD results were validated with the one dimensional theoretical predictions and the exit Mach number of the baseline configuration was found to differ by 3.17% from the theoretical value of 3.65, showing good agreement. The nozzle is in an overexpanded condition in air and exhibits oblique shock structures in the exhaust plume as seen in such a flow with the area ratio of 8.97 at this condition.

The quantitative comparison between the two configurations indicates that the gimbal joint gap reduces the exit Mach number from 3.766 to 3.512, corresponding to a reduction of 6.74%, and the exit velocity from 2328 m/s to 2286 m/s, representing a reduction of 1.79%. The reductions suggest that part of the flow energy is lost because of increased turbulence, flow deflection, and recirculation zones within the gap region. The static pressure and temperature distributions are, however, virtually identical in the two configurations, implying that the gimbal gap effect is primarily kinematic in nature.

In general, the results validate the conclusion that aerodynamic losses caused by a relatively small geometric discontinuity like a gimbal joint

gap are measurable. The results presented here have shown that the presence of structural discontinuities in rocket propulsion applications is important to consider in the design and optimization of thrust vector control systems. The 2D axisymmetric approximation used here is numerically efficient and is applicable to the parametric study shown here, however it is not necessarily representative of a real simulation in 3D. Azimuthal non-uniformity in the flow field, asymmetric flow separation patterns and the three-dimensional recirculation zones that may exist in an actual nozzle with a geometrically discrete gap feature are examples of conditions not captured by the 2D axisymmetric model. Moreover, gimbal deflection causes an off-axis loading condition, which is inherently not axisymmetric, and therefore cannot be modeled in an axisymmetric fashion.

Future research could involve simulations of the 3D case, transient effects in the flow, and the effects of changing gap sizes to gain further insight into the aerodynamic performance of gimbaled nozzle systems. In particular, 3D simulations of the gimbaled nozzle under gimbal angle deflection would allow the full resolution of three-dimensional flow effects that are inherently outside the scope of the present axisymmetric model.

Acknowledgment

This work was funded by the Committee of Science of the Ministry of Science and Higher Education of the Republic of Kazakhstan, grant number BR249008/0224.

Author Contributions: Conceptualization, A.S.T., M.K.O. and N.M.S.; methodology, A.S.T., M.K.O., T.K.Z., A.Y.D. and N.M.S.; software, A.S.T. and M.K.S.; validation, A.S.T. and A.Y.K.; formal analysis, A.Y.K.; investigation, M.K.O. and T.K.Z.; resources, A.S.T.; data curation, A.S.T.; writing-original draft preparation, A.S.T., M.K.O. and A.Y.D.; writing-review and editing, A.Y.K.; visualization, M.K.S.; supervision, A.S.T. and M.K.O.; project administration, A.S.T. All authors have read and agreed to the published version of the manuscript.

References

[1] Yaravintelimath, A., B. N. Raghunandan, and J. A. Moríñigo. "Numerical prediction of nozzle flow separation: Issue of turbulence modeling." *Aerospace Science and Technology* 50 (2016): 31–43.

[2] Dubrovskyi, I. and V. Bucharskyi. "Devising a method to design supersonic nozzles of rocket engines by using numerical analysis methods." *Eastern-European Journal of Enterprise Technologies* 126, no. 1 (2023): 61–67.

[3] Dintayev, A., M. Omarbayev, D. Tastaibek, A. Komekbayev, and R. Zhunussov. "Selection of a propellant feed system for the LPRE of a small upper stage." *International Journal of Mathematics and Physics* 16, no. 2 (2025):. doi.org/10.26577/ijmph.20251623

[4] Zmijanovic, V., V. Lago, M. Sellam, and A. Chpoun. "Thrust shock vector control of an axisymmetric conical supersonic nozzle via secondary transverse gas injection." *Shock Waves* 24, no. 1 (2014): 97–111.

[5] Sopegno, L., P. Livreri, M. Stefanovic, and K. P. Valavanis. "Thrust vector controller comparison for a finless rocket." *Machines* 11, no. 3 (2023): 394.

[6] Shimizu, T., M. Kodera, and N. Tsuboi. "Internal and external flow of rocket nozzle." *Journal of Earth Simulator* 9 (2008): 19–26.

[7] Hu, H., X. Gao, Y. Gao, and J. Yang. "Shock wave and aeroelastic coupling in overexpanded nozzle." *Aerospace* 11, no. 10 (2024): 818.

[8] Nair, P. P., A. Suryan, and H. D. Kim. "Computational study on reducing flow asymmetry in over-expanded planar nozzle by incorporating double divergence." *Aerospace Science and Technology* 105 (2020): 105790. https://doi.org/10.1016/j.ast.2020.105790

[9] Duronio, F., C. Villante, and A. De Vita. "Under-expanded jets in advanced propulsion systems — a review of latest theoretical and experimental research activities." *Energies* 16, no. 17 (2023): 6433. https://doi.org/10.3390/en16176433

[10] Khare, S. and U. K. Saha. "Rocket nozzles: 75 years of research and development." *Sādhanā* 46, no. 2 (2021): 1–39. https://doi.org/10.1007/s12046-021-01635-9

[11] Zivkovic, S., M. Milinovic, N. Gligorijevic, and M. Pavic. "Experimental research and numerical simulations of thrust vector control nozzle flow." *Aeronautical Journal* 120, no. 1229 (2016): 1153–1174. https://doi.org/10.1017/aer.2016.48

[12] Banazadeh, A., F. Saghafi, M. Ghoreyshi, and P. Pilidis. "Experimental and computational investigation into the use of co-flow fluidic thrust vectoring on a small gas turbine." *The Aeronautical Journal* 112, no. 1127 (2008): 17–25. https://doi.org/10.1017/s0001924000001950

[13] McBride, B. J. and S. Gordon, *Properties of Individual Species*, ser. NASA/RP-1311-Part-2. Cleveland, OH: NASA Glenn Research Center, 2002.

[14] Sutherland, W. "The viscosity of gases and molecular force." *Philosophical Magazine Series 5* 36, no. 223 (1893): 507–531. https://doi.org/10.1080/14786449308620508

[15] Yu, Y., M. Shademan, R. M. Barron, and R. Balachandar. "CFD study of effects of geometry variations on flow in a nozzle." *Engineering Applications of Computational Fluid Mechanics* 6, no. 3 (2012): 412–425.

[16] Hadjadj, A. and M. Onofri. "Nozzle flow separation." *Shock Waves* 19, no. 3 (2009): 163–169. https://doi.org/10.1007/s00193-009-0209-7

[17] Martelli, E., L. Saccoccio, P. P. Ciottoli, C. E. Tinney, W. J. Baars, and M. Bernardini. "Flow dynamics and wall-pressure signatures in a high-Reynolds-number overexpanded nozzle with free shock separation." *Journal of Fluid Mechanics* 895 (2020):. https://doi.org/10.1017/jfm.2020.280

[18] Mane, S. "Nozzle flow separation phenomena and control for different conditions." *REST Journal on Advances in Mechanical Engineering* 1, no. 3 (2022): 10–15. https://doi.org/10.46632/jame/1/3/2

Information about authors

A.S. Toleubay *– researcher, JSC National Center for Space Research and Technology, Almaty, Kazakhstan, e-mail: aruzhan-toleubay4@gmail.com*
M.K. Omarbayev *– researcher, JSC National Center for Space Research and Technology, Almaty, Kazakhstan*
M.K. Suleimenov *– researcher, JSC National Center for Space Research and Technology, Almaty, Kazakhstan*
T.K. Zhakenova *– researcher, JSC National Center for Space Research and Technology, Almaty, Kazakhstan*
A.Y. Dintayev *– researcher, JSC National Center for Space Research and Technology, Almaty, Kazakhstan*
N.M. Spandiyar *– researcher, JSC National Center for Space Research and Technology, Almaty, Kazakhstan*
A.Y. Komekbayev *– researcher, Almaty University of Energy and Communications named after Gumarbek Daukeev, Almaty, Kazakhstan, Almaty, Kazakhstan*